Simulation and analysis of the performance map of a micro-ORC-turbine - Comparison with measurements

Cite as: AIP Conference Proceedings **2189**, 020022 (2019); https://doi.org/10.1063/1.5138634
Published Online: 22 November 2019

Philipp Streit, Tobias Popp, and Andreas P. Weiß

Simulation and Analysis of the Performance Map of a Micro-ORC-Turbine - Comparison with Measurements

Philipp Streit[1, a)] and Tobias Popp[1, b)] and Andreas P. Weiß[1, c)]

[1]OTH Amberg-Weiden, Center of Excellence for Cogeneration Technologies, *Kaiser-Wilhelm-Ring 23, 92224 Amberg, Germany*

[a)]Corresponding author: ph.streit@oth-aw.de
[b)]to.popp@oth-aw.de
[c)]a.weiss@oth-aw.de

Abstract. The paper deals with the CFD simulation and investigation of an axial Micro-ORC-Turbine, running with the working fluid hexamethyldisiloxane (MM). The CFD results are compared to the experimental results of the turbine, which were determined at the Center of Energy Technology at the University of Bayreuth. The simulation software Fine/Turbo by NUMECA was used for the meshing and simulation of the turbine. After the mesh studys and optimization of the geometry grid have been carried out, different pressure ratios and rotational speeds have been simulated. The simulated efficiency maps were compared to the experimentally determined efficiency maps. The simulated efficiency characteristics show principally a very similar turbine operating behavior to the measured ones. However, the simulated efficiencies are about 2 to 3 percentage points higher than the measured data. Through the detailed analysis of the blade-to-blade flow fields, it was possible to plausibly trace the integral course of the efficiency curves. Thus, CFD turbine flow simulation proved to be a valuable tool to predict the efficiency characteristics of a Micro-ORC-Turbine.

INTRODUCTION

The Organic Rankine Cycle or ORC process is currently developing into an interesting technology for industrial companies as a result of the environmental protection and energy policy, which becomes more and more important [1]. The fact that the ORC can efficiently use heat sources of low or medium temperature levels makes it superior over conventional processes such as the Clausius Rankine Cycle. Simulations serve as a tool for the confirmation or comparison of the theoretical design with the expected performance of the turbine in its real application. Computational Fluid Dynamics (CFD) cannot replace the measuring equipment, but can significantly reduce the number of required experiments and the total cost of development [2]. The present paper demonstrates, how comparable the performance map data of a simulation with a simplified geometry is against the experimentally determined data from the real turbine. The software Fine/Turbo by NUMECA was used for the simulations [5]. For the rotor stator interface, a full non-matching frozen rotor was chosen. As turbulence model, the Spalart-Allmaras model was applied.

18th Conference of Power System Engineering, Thermodynamics and Fluid Mechanics
AIP Conf. Proc. 2189, 020022-1–020022-10; https://doi.org/10.1063/1.5138634
Published by AIP Publishing. 978-0-7354-1936-0/$30.00

METHODOLOGY

Geometry Simplification

In comparison to the geometry of the experimentally analyzed Micro-ORC-Turbine, some simplifications to the simulated model were implemented. These modifications were performed, to reduce the computational effort and the calculation time of the computer used for the simulations.

(a)

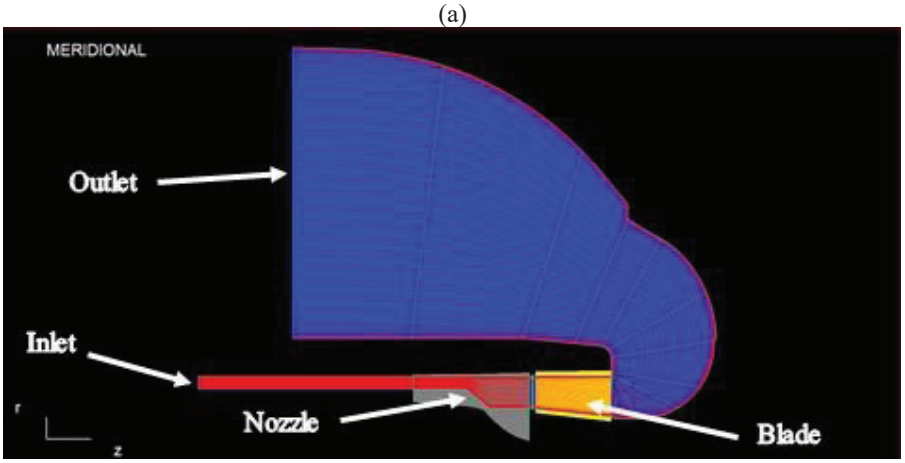

(b)

Figure 1. Comparison of the real (a) and simplified, simulated geometry (b) of the micro turbine

Figure 1 (a) shows two pictures of the rotor in its installed (left) and single (right) condition, where the gap between the rotor and the housing as well as the shroud around the blades can be seen. Figure 1 (b) demonstrates the meridional cut of the simulated turbine with its most important components marked with white arrows. Because the turbine wheel is directly mounted on the generator shaft and the nozzles are located on the opposite side, a 180°-deflection is needed at the turbine outlet. The most significant simplification was carried out at the blade geometry, where in the simulation, the shroud at the top of the blades and the gap of the real turbine were ignored. These simplifications become obvious, looking at the yellow blade geometry in Fig. 1. (b). Here, the tip of the blade is directly connected to the shroud surface of the flow channel.

1-D Calculation Turbine Data

Table 1 depicts the 1D design data of the Micro-ORC-Turbine. Boundary Conditions which led to the main turbine design data listed in this table are: mass flow rate of MM 0.32 kg/s; turbine inlet pressure 6.0 bar; inlet temperature: 176 °C; turbine back pressure 0.32 bar [3].

TABLE 1 Turbine main design data

Parameter	Unit	Micro-ORC-Turbine
working fluid	-	Hexamethyldisiloxane (MM)
wheel diameter D_{mean}	mm	120
rotational speed n	rpm	24,000
degree of admission ε	%	100
pressure ratio PR (ts)	-	18.75
degree of reaction r	%	0
nozzle exit Mach number Ma_1	-	2.11
rotor relative Mach number Ma_{r1}	-	1.14
expected shaft power	kW	12-13
predicted total to static isentropic efficiency (1D loss model) $\eta_{ts,1D}$	%	67.0

Mesh Study

To assess the quality of the mesh, studies of different grid accuracies were implemented and the different results were compared to each other. Figure 2 shows the inlet and outlet mass flow rate over different grid point numbers for a pressure ratio of 15.3, where a higher grid point number means a finer mesh. It becomes obvious, that the mass flow rate for both inlet and outlet flattens out at about 252 g/s for a grid point number of 13.3 Million. With a higher number of grid points, no further changes of the mass flow rate occur. With the information from Fig. 2, it becomes apparent, that the ideal number of grid points is at about 13.3 Million. Therefore, the mesh with 13.3 Million grid points is the most efficient one, but still delivers the most realistic results. The experimental measurements showed mass flow rates even lower than 252 g/s. Thus, the decrease in mass flow rate with increasing number of grid points corresponds to an improvement of accuracy.

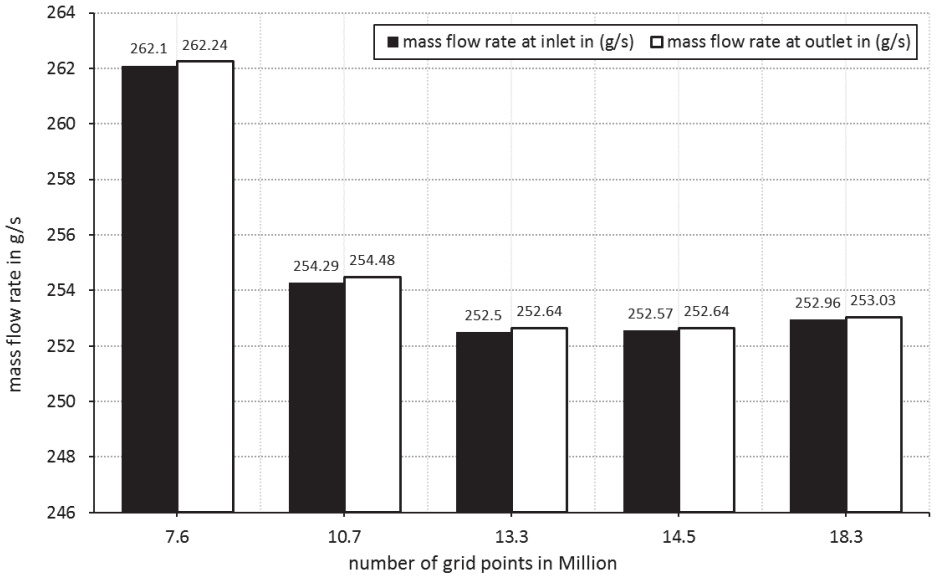

Figure 2. Mass flow rate through the turbine as a function of number of grid points

RESULTS

Corrected Mass Flow Rate

In order to enable a proper comparison of the mass flow rate of the different analyzed pressure ratios, the mass flow rates were normalized via the corrected mass flow rates. The corrected mass flow rate $\dot{m}_{corr}$ is calculated as followed:

$$\dot{m}_{corr} = \frac{\dot{m} * \sqrt{T_{t,in}}}{p_{t,in}} \tag{1}$$

Using Equation 1, the mass flow rates of the different pressure ratios are standardized by means of the total inlet temperature $T_{t,in}$ and the total inlet pressure $p_{t,in}$.

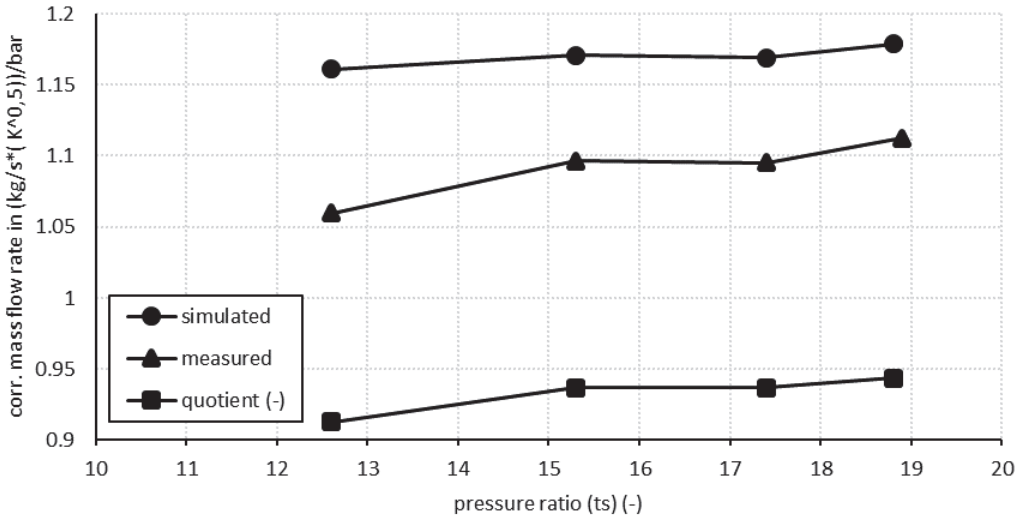

Figure 3. Corrected mass flow rates of the measured and simulated turbine and quotient as a function of pressure ratio

Figure 3 compares the corrected mass flows rates of the simulation and the measurement over the pressure ratio. In addition, a quotient of the two curves was formed, which represents the deviation of the lines from each other. The divergences of the graphs decrease with a higher pressure ratio. This is evident from the quotient, which rises with increasing pressure ratio. Thus, the deviation between the two different mass flow rates decreases.

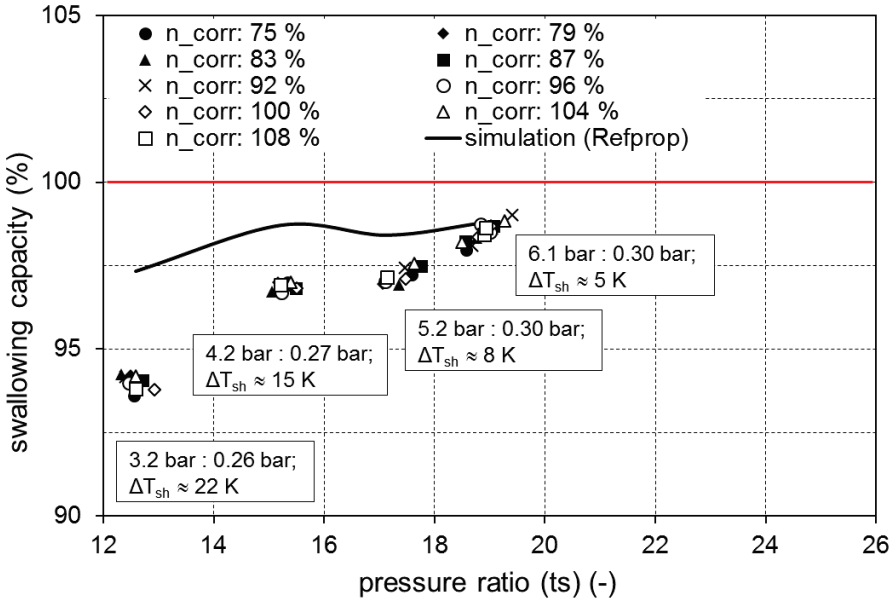

Figure 4. Swallowing capacity as a function of pressure ratio (ts) [3]

Figure 4 compares, just as Fig. 3, the experimental results for a value of mass flow rate as a function of pressure ratio with results from a simulation 1-D model. While in Fig. 3 the results for the corrected mass flow rate were analyzed, in Fig. 4 the swallowing capacity is considered. The swallowing capacity is calculated by normalizing the corrected mass flow rate by its design point value. As simulation model a 3-D CFD analysis was used in Fig. 3, compared to a 1-D model in Fig. 4. In Fig. 4, similar to Fig. 3, the deviation between the experimentally determined and the simulated results decreases with higher pressure ratios. Both, the CFD simulation with its fluid model and the design tool for the 1-D calculation apply the REFPROP database. Therefore, the divergences between the measurements and the simulations might be explained by REFPROP not being able to map the fluid data properly [4].

Performance Maps

To compare the total-to-static isentropic efficiencies of the simulation and the measurements, performance maps for the different pressure ratios were created. It should be mentioned that the design point of the turbine is at a pressure ratio of approximately 18.8 and a rotational speed of 24,000 rpm (see Table 1). For the simulated curves, only six specific rotational speeds were calculated, as this number was considered sufficient for comparison with the measured curves. In addition, a further point was simulated at 28,000 rpm, which was not included in the measurements of the real turbine. This point was added to the simulation, since there was no declining trend visible at 26,000 rpm. With this additional data point, the expected decrease in efficiency after reaching its peak value was observed.

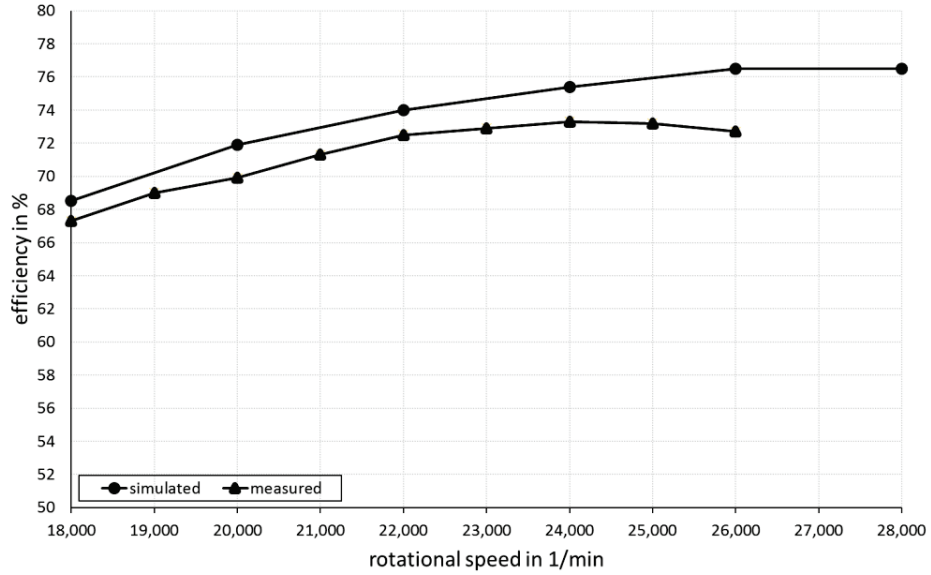

Figure 5. Total-to-static isentropic efficiency as a function of rotational speed at a pressure ratio (ts) of 18.8

Figure 5 shows the total-to-static isentropic efficiencies of the simulated and measured turbine at the Micro-ORC-Turbine's design pressure ratio of 18.8. The course of the simulated curve over the entire range of rotational speed is always approx. 2 – 4 % above the curve of the experimental results. Furthermore, it becomes clear that the point of maximum efficiency in the simulation occurs at a rotational speed that is about 2,000 rpm higher than the measured maximum efficiency. The deviation of the rotational speed with the highest efficiency and the constant deviation of 2 to 4 % for the whole considered range can be explained by the mentioned significant simplification of the turbine geometry. Furthermore, the entire disc of the rotor is not simulated in the calculation and some of the frictional influences e.g. caused by bearings, are not taken into account. These circumstances explain the positive deviation between the simulated and measured curves. The occurrence of points of maximum efficiency at different rotational speeds can be explained by the missing gap and therefore fewer bypass losses for the modelled geometry. These reduced flow losses in the simulation result in a higher flow rate through the impeller compared to the real geometry. This leads to a higher idling speed and thus to higher rotational speed of the maximum efficiency.

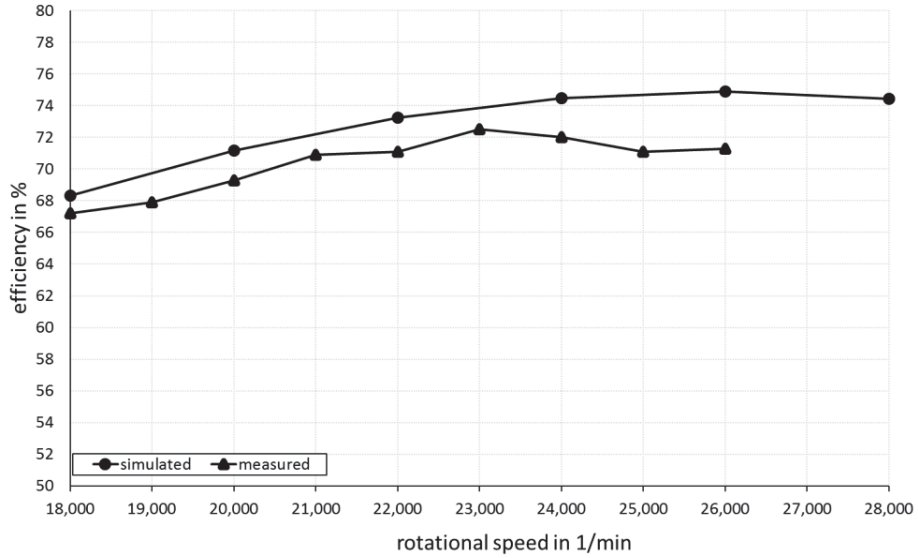

Figure 6. Total-to-static isentropic efficiency as function of rotational speed at a pressure ratio (ts) of 15.3

Figure 6 shows the performance maps at a pressure ratio of 15.3. Here, no major differences compared to the results for the design pressure ratio can be seen. In total, both curves are somewhat lower and flatter than the curves at the higher pressure ratio. The drop in efficiency from 26,000 to 28,000 rpm for the simulated results is more pronounced compared to the results for the design pressure ratio.

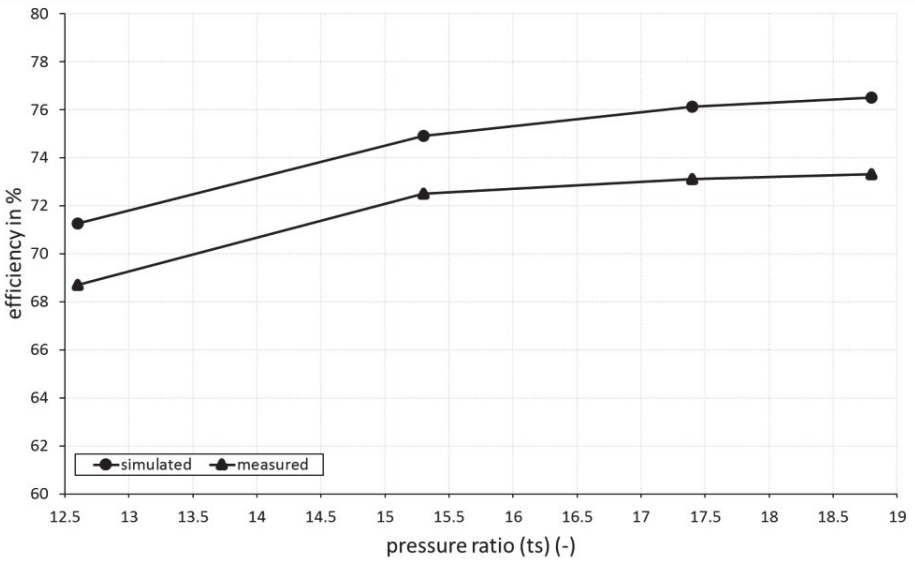

Figure 7. Maximum total-to-static isentropic efficiency at different pressure ratios (ts)

The maximum simulated and measured total-to-static isentropic efficiencies at a certain rotational speed of the simulated and measured turbine over the different pressure ratios are depicted in Fig. 7. The maximum efficiency steadily rises up to the design pressure ratio of 18.8 and reaches its maximum in the considered range for both of the curves. The simulated maximum efficiencies are always approx. 2 – 3 % higher than the course of the measured efficiencies by the simulation. Thus, this diagram shows that it is possible to plausibly trace the integral course of the maximum measured efficiencies by the simulations. However, the simulated maximum efficiencies are too high due to the simplification across all the pressure conditions.

Blade-to-Blade Views

To see the biggest differences in the blade-to-blade views, a comparison of the lowest measured (18,000 rpm) and the highest simulated (28,000 rpm) rotational speed at a fixed pressure ratio (18.8) is performed.

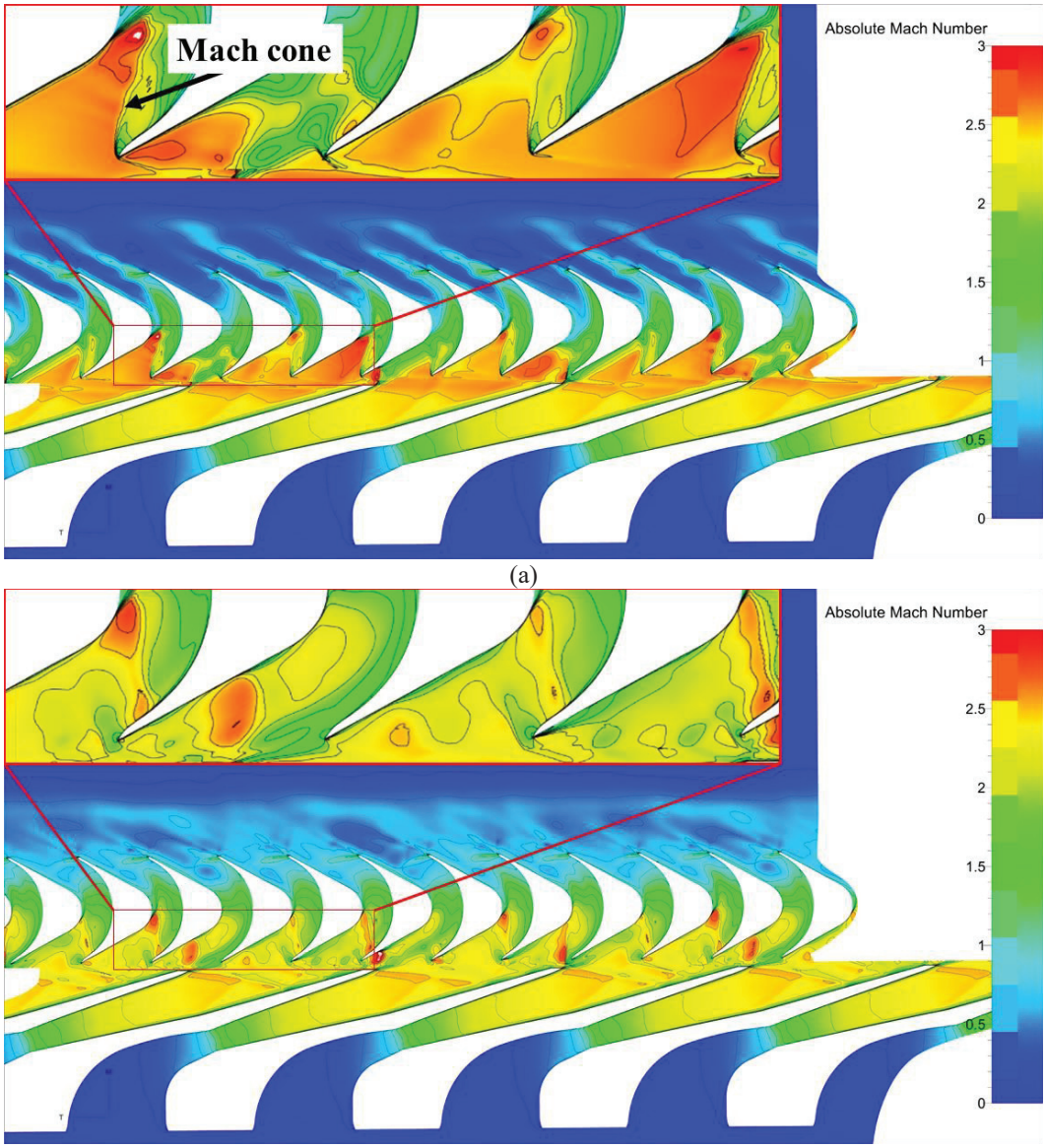

Figure 8. Absolute Mach number at pressure ratio 18.8 for 18,000 rpm (a) and 28,000 rpm (b)

Figure 8 shows the absolute Mach number at a fixed pressure ratio of 18.8 for two different rotational speeds. In the upper area of both illustrations, a certain area is enlarged. The Laval nozzle accelerates steadily and as designed to supersonic speed. In the upper picture, with lower rotational speeds, higher absolute flow velocities occur in the inlet area of the blades compared to the lower picture. Comparing the enlarged images, it becomes obvious that the Mach cone has greater influence if the rotational speed is lower and thus the relative velocity is higher. Especially in the left area of the upper zoom in Fig. 8 (a), the clear differentiation of the cone is visible, whereas it is no longer recognizable at higher rotational speeds in the lower zoom in Fig. 8 (b). Furthermore it becomes clear, that the cone forms vortices, which lead to pointed converging speed increases. These speed peaks can be recognized in every fully

loaded blade and lead to the fact, that shortly after these peaks, the flow separates from the blade suction surface. The difference of the flow separation becomes clear in this example, since in Figure 8 (a), the flow clearly separates from the geometry, whereas in Figure 8 (b) at a higher rotational speed, the flow is better deflected. These differences are also noticeable in the area behind the rotor, whereas in Figure 8 (b), at 28,000 rpm, there is a much more homogenous velocity field behind the rotor than in Figure 8 (a).

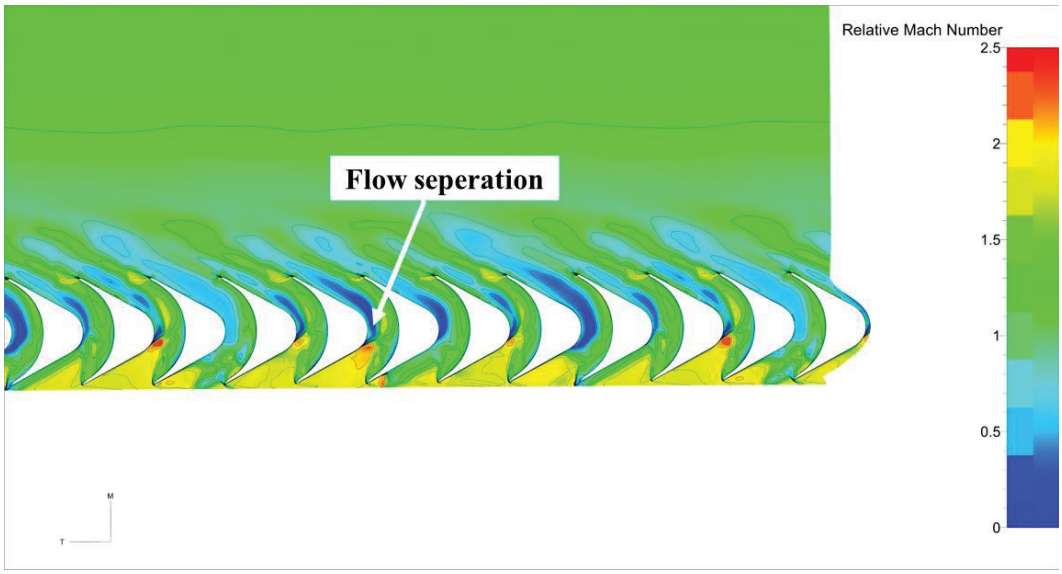

(a)

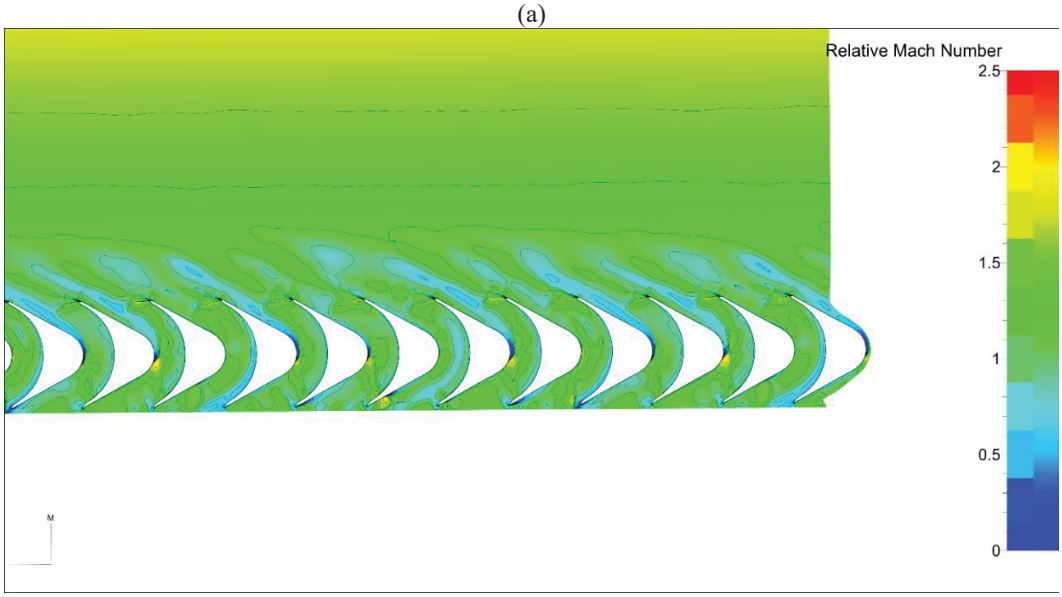

(b)

Figure 9. Relative Mach number at pressure ratio 18.8 for 18,000 rpm (a) and 28,000 rpm (b)

The above-mentioned separation is also noticeable in Fig. 9, which shows the relative Mach number at the same pressure ratio and rotational speeds as shown in Fig. 8. The dark blue areas in Fig. 9 (a), representing the flow separation, indicate that the turbine does not operate at its design point. In this case, the Spalart-Allmaras turbulence model cannot correctly simulate the areas behind the flow separation and therefore distorts the results of the simulation. In Fig. 9 (b), in contrast, the flow clearly follows the geometry of the blade. These flow differences also have an effect on the efficiency of the considered rotational speeds with a difference of about 8 percentage points. The entry relative velocity from the nozzle into the blade also shows clear deviations, whereby the velocity at the lower

rotational speed is almost Mach 0.5 higher than at the higher rotational speeds. This higher relative velocity at a rotational speed of 18,000 rpm has a corresponding effect on the Mach cone already described. The Mach number continues to increase in the area after the rotor up to the outlet of the geometry, which cannot be explained logically, since the velocities in the absolute system in this area are clearly in the subsonic range. This velocity course may be caused by the fact that the area after the rotor is bent by 180° and the solver may have problems to calculate the relative velocity of the flow in this area. Furthermore, the representation in CFView could encounter problems due to this bend and therefore assumes an increasing speed towards the outlet of the turbine housing.

DISCUSSION

The comparison of the performance maps of the simulated and measured turbine show that the deviations are mainly in the upper range of the considered rotational speeds, which can be explained by the strong simplification of the geometry in the simulation. All other deviations are within comprehensible limits and a comparison of the actually measured and simulated curves is therefore reasonable. The deviations of the mass flow rates from the measured turbine, which are present in every simulation, could not be eliminated even by the calculation of the reduced mass flow rate. This is why it is assumed that the deviations are at least partly caused by the fluid model tables from REFPROP and not by incorrect settings in the simulation software or by tolerances in the geometry. Through the detailed analysis of the blade-to-blade flow fields, it was possible to plausibly trace the integral course of the efficiency curves.

CONCLUSION

Due to the circumstances described above, it is conceivable that in the future even simulations of simplified geometries of ORC turbomachineries can be used to draw conclusions about the approximate course of the efficiency map. This allows for an assessment, whether the turbomaschinery is operating at the theoretical design point with the highest efficiency, before the turbine is manufactured. The simplified geometry is also sufficient for the evaluation of the nozzle and the blade surfaces in the blade-to-blade cut, since no changes are performed to the real turbine geometry in these areas. In future, simulations should be performed, in which the geometry is meshed as realistic as possible and the obtained results are compared to the values obtained in this paper. Thus, an estimation of the extent of the obtained additional information would be possible. This would enable a decision if a more precise calculation would be necessary or if a simpler meshed geometry would be more efficient and/or sufficient for the analysis. The focus of additional investigations could also lie on other simulation values, such as axial force, torque or power, which were not relevant in this paper.

ACKNOWLEDGMENTS

The work has been supported by the grant project Ziel - ETZ INTERREG V Project 53 Grenzüberschreitendes F&I Netzwerk für Energieeffizienz und Kraft-Wärme- (Kälte)-Kopplung / Preshranicní sít pro výzkum a inovace v oblasti energetické úcinnosti a kombinované výroby tepla a elektriny (2016 - 2020).

REFERENCES

1. F. Campana, et al. *ORC waste heat recovery in European energy intensive industries: Energy and GHG savings.* Energy Conversation and Management, Bd. 76, p. 244-252, Dec. 2013
2. S. Lecheler, *Numerische Strömungsberechnung.*(Springer Verlag, Wiesbaden, 2011), p. 1-3
3. Andreas P. Weiß, Tobias Popp, Jonas Müller, Josef Hauer, Dieter Brüggemann, Markus Preißinger. *Experimental characterization and comparison of an axial and a cantilever micro-turbine for small-scale Organic Rankine Cycle.* Applied Thermal Engineering, Volume 140, p. 235-244, 25. June 2018
4. NIST-REFPROP, *https://www.nist.gov/srd/refprop* (retrieved on 04.04.2019)
5. NUMECA-Online, *https://www.numeca.com/home* (retrieved on 09.04.2019)